Supporting Information for

Chemiresistive Carbon Nanotube Sensors for *N*-nitrosodialkylamines

Maggie He[1], Robert G. Croy[1,2], John M. Essigmann[1,2] and Timothy M. Swager*[1]

[1] Department of Chemistry, Massachusetts Institute of Technology, 77 Massachusetts Avenue, Cambridge, MA 02139, USA

[2] Departments of Biological Engineering and Center for Environmental Health Sciences, Massachusetts Institute of Technology, 77 Massachusetts Avenue, Cambridge, MA 02139, USA

*Corresponding author: tswager@mit.edu

Table of Contents

1. General information

Materials. Purified SWCNTs (UPT-200 series, mixture of metallic and semiconducting tubes) were obtained from Nano-C. DWCNTs with 50–80% carbon basis (O.D. × I.D. × length: 5 nm × 1.3–2.0 nm × 50 μm), FWCNTs with ≥95% carbon content (D × L: 2.5–3 nm × 2–6 μm), MWCNTs with >95% content as MWCNTs (O.D. × I.D. × length: 7–15 nm × 3–6 nm × 0.5–200 μm), Semiconducting SWCNTs enriched in (7,6) chirality, **(7,6)-SWCNTs**, with >90% carbon content and ≥77% carbon as SWCNTs (0.7–1.1 nm diameter) were purchased from Sigma-Aldrich. Meso-tetraphenylporphine was purchased from Alfa Aesar. NDMA was prepared following the procedures described by Heath and Mattocks.[1] Briefly, sodium nitrite in water was slowly added to a solution of dimethylanime in water and acetic acid. After cooling, 10 N NaOH was added and the solution was extracted four times with Et_2O. The ether solution was dried over Na_2SO_4 and NDMA was isolated as a pale-yellow liquid by fractional distillation (b.p. 148–149 °C). HRMS (ESI) calc for $C_2H_7N_2O^+$ $[M+H]^+$ 75.0480, found 75.0056. ^{1}H NMR (300 MHz, $CDCl_3$) δ 3.06 (s, 3H,Me *cis*), 3.76 (s,3H,Me *trans*). The NMR assignments are in agreement with those reported for NDMA.[2] Aliquots of NDMA were packaged in sealed ampules under Ar gas and stored at –20 °C. Contaminated glassware was treated with a solution of concentrated hypochlorite containing strips of aluminum foil overnight to destroy nitrosamines.[3] NDEA was purchased from TCI. NDBA and meso-tetraphenylporphyrin iron(III) chloride were purchased from Sigma-Aldrich. All CNTs and chemicals were used as received.

Instrumentation. ^{1}H NMR spectra were recorded on a Varian Mercury 300 spectrometer or a Bruker-ADVANCE 400 spectrometer as indicated. Mass spectrometry was carried out on an Agilent single quadrupole mass spectrometer. UV-Vis absorption spectra were measured with 10 mm path length quartz cuvettes using an Agilent Cary 4000 Series UV-Vis spectrophotometer. Transmission FTIR spectra were collected using a Thermo Scientific Nicolet 6700 FT-IR and a Specac Omni-Cell liquid transmission cell with a pair of NaCl plate window. IR samples were prepared by either dropcasting neat *N*-nitrosamines, air drying a solution of *N*-nitrosamine porphyrin complex in CH_2Cl_2 or vacuum drying a metal free porphyrin in 1,2-dichlorobenzene onto a NaCl plate window. The salt plate containing analytical sample was fitted into the liquid cell to contain and prevent exposure to toxic chemicals during FTIR measurements.

2. Synthesis of porphyrins and pyridyl functionalized carbon nanotubes

4-Pyridyl functionalized (7,6)-SWCNTs were synthesized using the iodonium salt method with a degree of functionalization of 1.4 and 1.8 pyridyl groups per 100 CNT carbon atoms.[4,5] $[Cr(TPP)(ClO_4)]$[6–8], $[Mn(TPP)(H_2O)_2]ClO_4$[6,9], $[Fe(TPP)(H_2O)_2]ClO_4$[10], $[Co(TPP)(H_2O)_2]$[11], $[Co(TPP)(H_2O)_2]ClO_4$[12], $[Ni(TPP)(H_2O)_2]$[13], $[Cu(TPP)(H_2O)_2]$[13] and $[Zn(TPP)(H_2O)_2]$[13] were synthesized according literature procedures.[14]

3. Sensor fabrication

Devices were prepared on gold electrodes with a shared reference counter electrode and 14 isolated working electrodes with a channel gap of 1 mm. Gold electrodes were fabricated by thermal evaporation of chromium (10 nm) followed by gold (100 nm) on microscope glass slides fitted with a custom stainless-steel mask. The glass slides were cleaned by sonication in isopropanol for 10 min, dried with N_2 and treated with UV-ozone for 10 min before thermal evaporation of metals.

Sensors were prepared by dropcasting a dispersion of CNTs in 1,2-dichlorobenzene (150 μg in 3 mL, sonicate for 1 h in a chilled water bath) with a micropipette onto the gap between working electrodes. The solvent was removed under vacuum. The drop-casting and solvent drying steps were repeated until a device resistance of 1–10 kΩ was achieved as measured with a multimeter. Selectors were applied to the device by dropcasting a solution of metalloporphyrin in 1,2-dichlorobenzene (1 mg/mL, 1 uL) on top of the CNTs followed by solvent removal under vacuum.

4. Sensing setup

The prepared device was inserted into an edge connector mounted on a solderless breadboard and enclosed with a custom PTFE enclosure containing a gas inlet and outlet. Gaseous analytes diluted in nitrogen or compressed air (2% relative humidity) were delivered to the sensing enclosure using a KIN-TEK gas generator system calibrated for *N*-nitrosamines and VOCs. The gold electrodes were connected to a PalmSens EmStat potentiostat with a MUX16 multiplexer applying a constant 0.1 V potential across the electrodes. The current on each electrode was recorded using PSTrace software (v. 5.5). The change in current was converted to the negative change in conductance ($-\Delta G/G_o$ (%) = $(I_o - I)/I_o \times 100\%$, where I_o is the initial current), which was taken as the device's response. All sensing experiments were carried in triplicate and the average of three sensor responses and standard deviations was reported. Note: *N*-nitrosamine gas mixtures from the gas generator were destroyed by bubbling the gas through a solution of cuprous chloride and hydrochloric acid.[15]

Analytes with ppm level concentrations were directly delivered from a gas generator. Concentrations at the ppb level were generated using the setup shown in **Figure S1**. The flow of analyte gas from the gas generator was reduced using a mass flow controller (MFC) and then diluted with an appropriate flow in order to reach the desired concentration. The gas was sampled into the sensing chamber using an air pump operating at 100 mL/min.

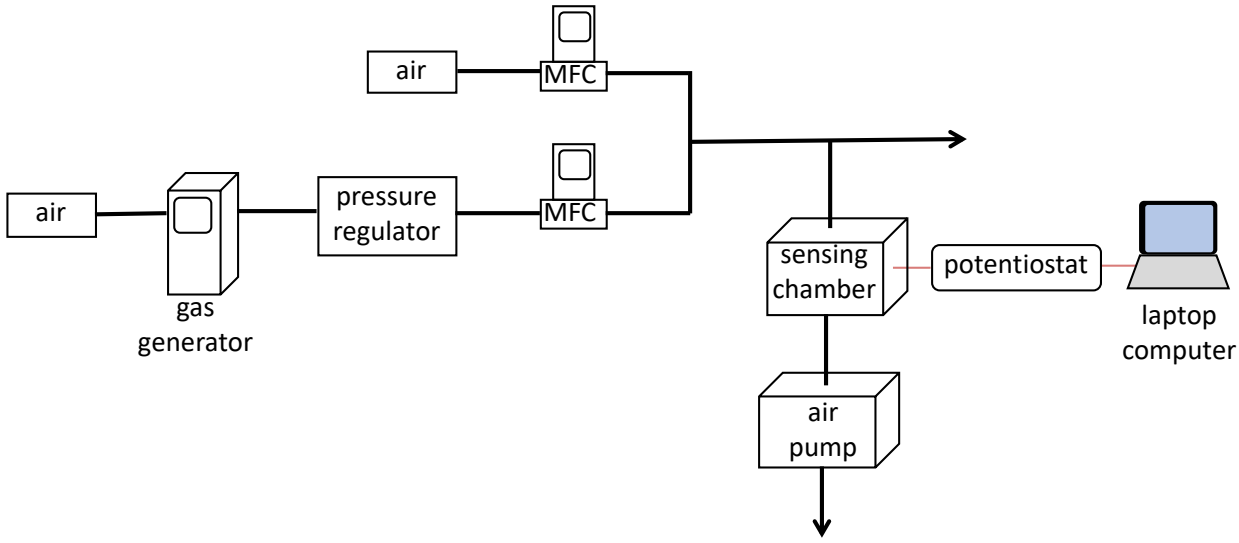

Figure S1. Experimental setup for ppb level gas analyte generation.

5. Sensor responses in N_2 and in air (2% RH)

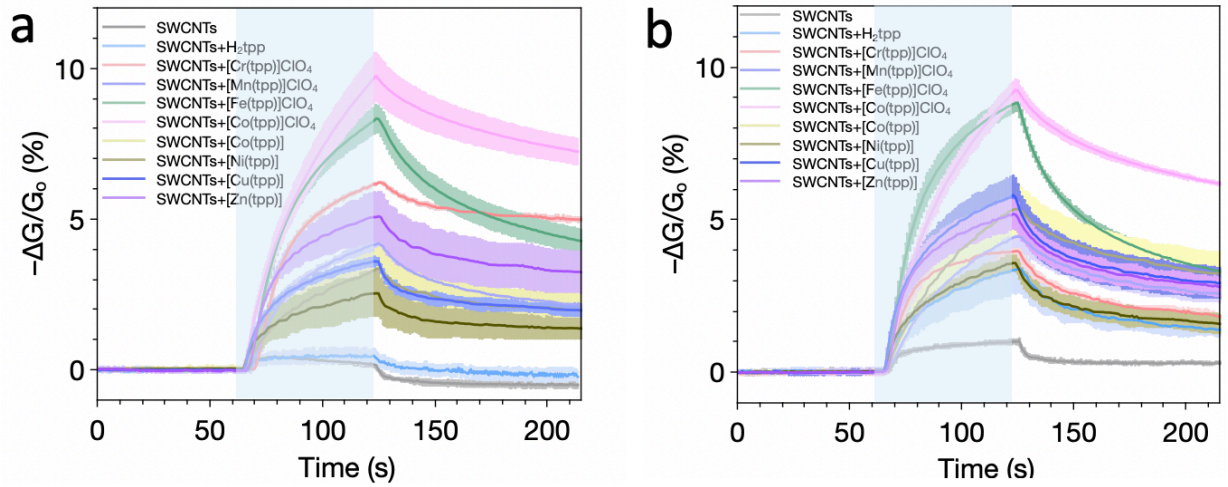

Figure S2. (a) Sensor responses to 100 ppm NDMA in N_2. (b) Sensor responses to 100 ppm NDMA in air (2% RH). Areas highlighted in light blue indicate exposure to NDMA.

6. Response of CNTs without selectors to NDMA

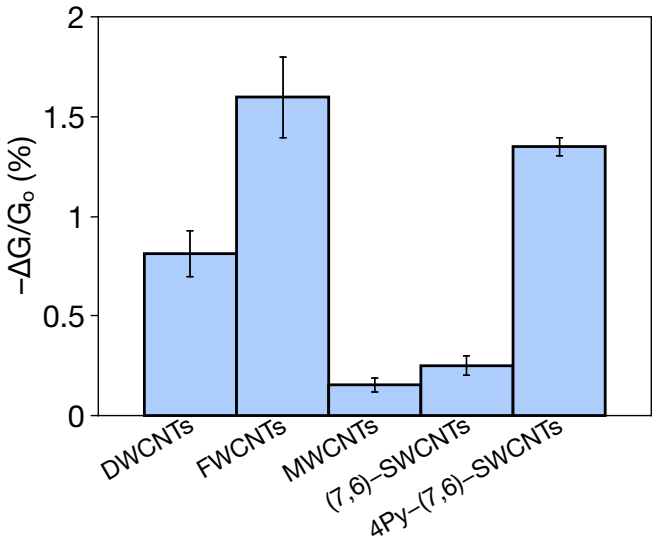

Figure S3. Control sensing responses of different types of CNTs without porphyrin selectors to 60 s of 100 ppm NDMA in air.

7. NMR spectra of H_2tpp, [Co(tpp)] and [Co(tpp)]ClO_4

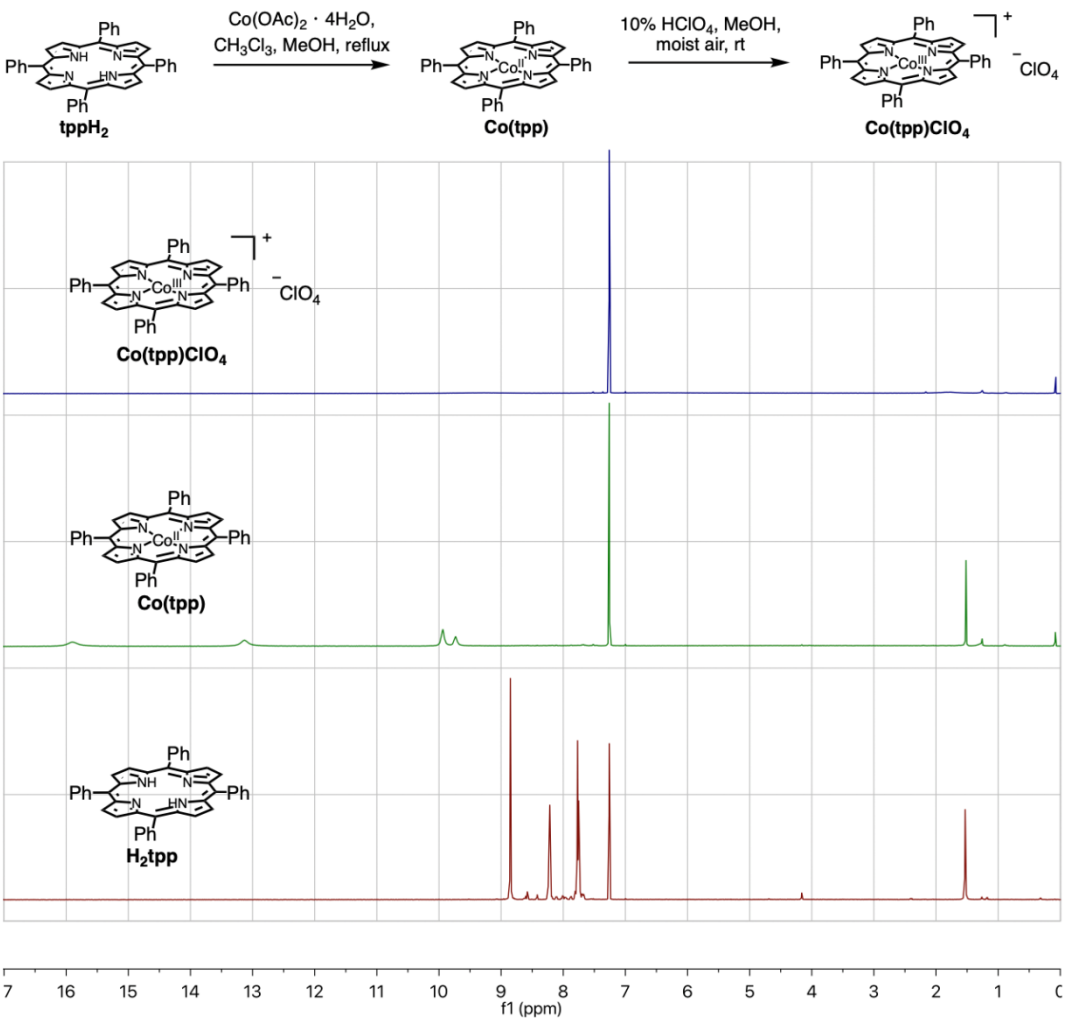

Figure S4. ^{1}H NMR spectra of H_2tpp, [Co(TPP)], [Co(TPP)]ClO_4 in $CDCl_3$. Aquo axial ligands in structures are omitted for clarity.

8. Binding experiments

UV-Vis titration. The binding constant of NDMA to [Co(tpp)]ClO_4 was determined by UV-Vis titration. Titration was carried out by addition of NDMA to a fixed concentration of [Co(tpp)]ClO_4 in CH_2Cl_2 at room temperature using a 10 mm pathlength cuvette. The binding constant was determined using Bindfit. A binding constant (K_a) of 91102 ± 26280 M^{-1} was determined using a 1:2 binding model. **Figure S5a** shows a good fit between experimental data and the calculated absorbance based on a 1:2 binding model. The residual plot (**Figure S5b**) shows randomly distributed data points above and below zero, indicating a good fit.

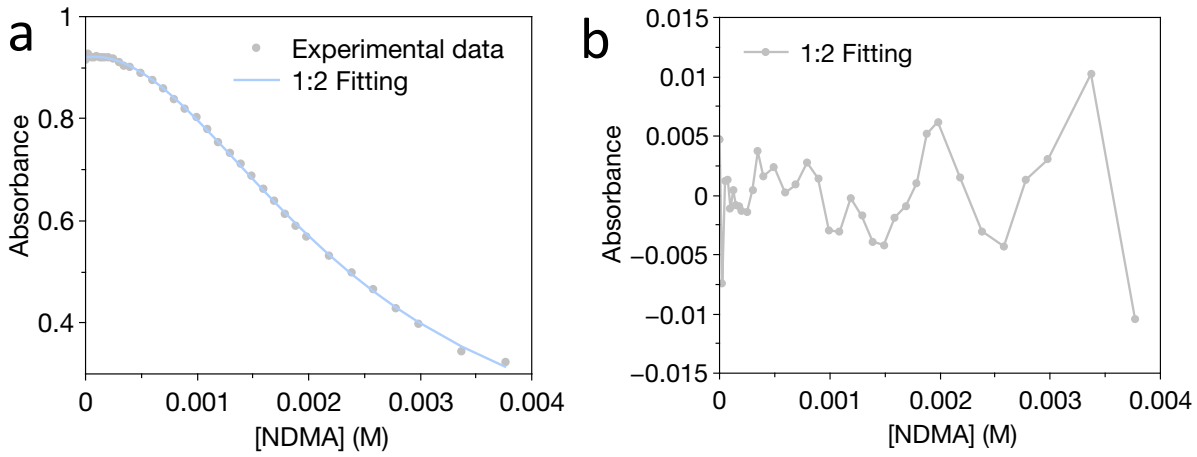

Figure S5. (a) Experimental absorbance and calculated absorbance based on a 1:2 binding model. (b) Residual plot.

Transmission FTIR. FTIR of pure *N*-nitrosamine and [Co(tpp)]ClO_4 are shown as a reference. Reference FTIR of *N*-nitrosamine and [Co(tpp)]ClO_4 complex (blue curve, **Figure S6**) are prepared by mixing 1 equivalent of [Co(tpp)]ClO_4 with two equivalents of *N*-nitrosamine in CH_2Cl_2. The resulting solution containing the complex was dropcasted onto a NaCl plate and air dried for FTIR measurement. Exposure of *N*-nitrosamine vapors to solid [Co(tpp)]ClO_4 on a NaCl plate produce the exact same FTIR as the complex formed in solution, indicating the binding of gaseous *N*-nitrosamines binding to [Co(tpp)]ClO_4 in the solid state. The appearance of a new IR stretch consisting of overlapping υ_{NN} and υ_{NN} stretches between 1230–1260 cm^{-1} is indicative of the binding of *N*-nitrosamines to the metal center of [Co(tpp)]ClO_4. The broad band around 1100 cm^{-1} belongs to the uncoordinated perchlorate anion.

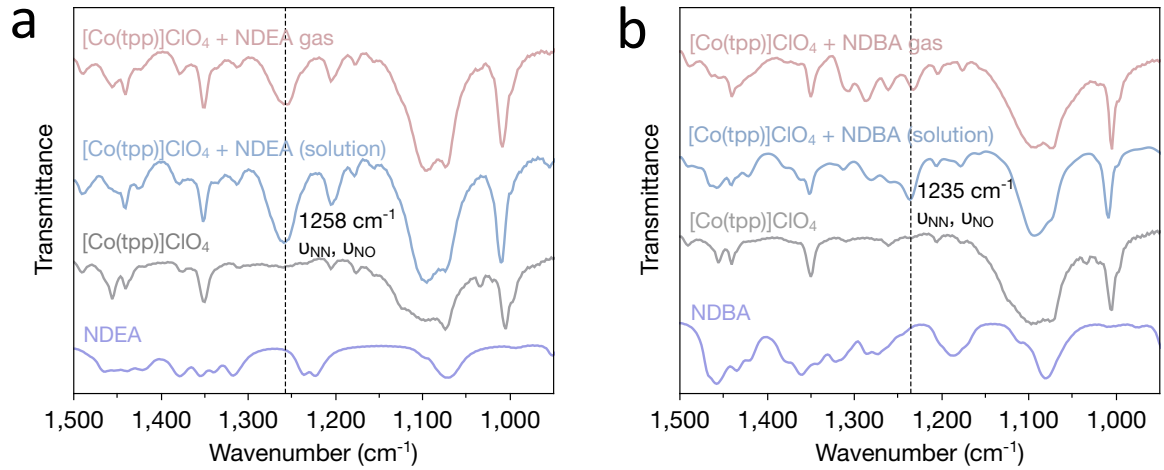

Figure S6. Transmission FTIR spectra demonstrating the binding of NDEA (**a**) and NDBA (**b**) gases to [Co(tpp)]ClO_4 in the solid state.

9. Device optimization

Sensing devices were first optimized by varying the device's resistance in the range of 1–10 kΩ, 10–100 kΩ and 100-1000 kΩ (**Figure S7**). The optimized resistance, 10–100 kΩ, were used to study the effect of different amount of [Co(tpp)]ClO_4 selector on the sensor's response. Lastly, we investigated devices with smaller channel gap between working electrodes. The analyte exposure time for all sensors was 60 s. The optimized device condition was determined to be 300 μm channel gap, 10–100 kΩ resistance range and 0.5 μL of 1 mg/mL [Co(tpp)]ClO_4 selector.

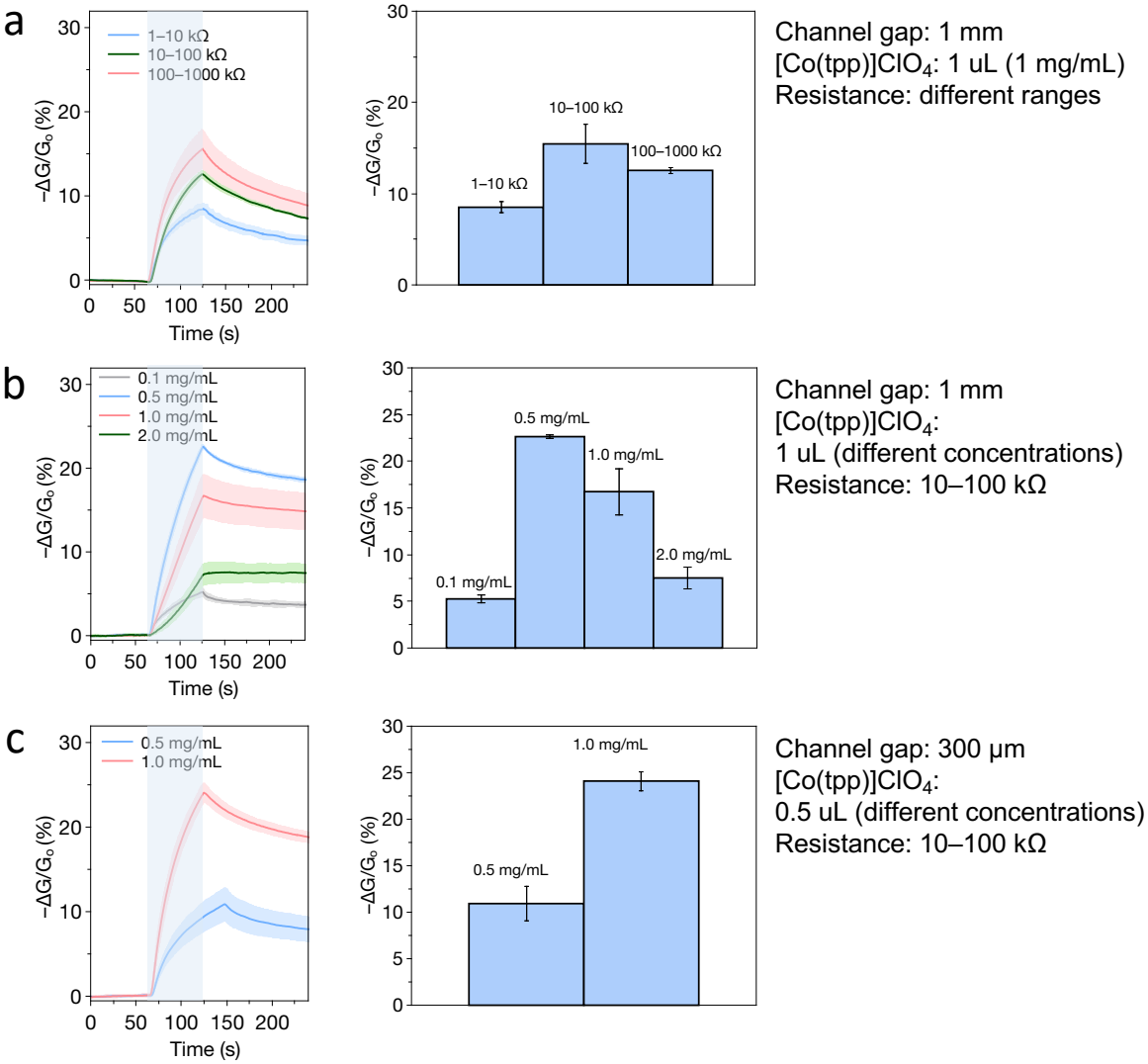

Figure S7. Device performance optimization. (**a**) Different device resistance ranges. (**b**) Different concentrations of [Co(tpp)]ClO_4 selector on 1 mm gap devices. (**c**) Different concentrations of [Co(tpp)]ClO_4 selector on 300 μm gap devices. The blue trace has an exposure time of 85 s. Areas highlighted in light blue indicate exposure to NDMA.

10. Sensing under controlled humidity

Controlled humidity in gas sensing was introduced by the setup outlined in **Figure S8**. The relative humidity was read by a VWR Traceable® Hygrometer. The sensors exhibit no significant change in response in the presence of different humidity levels from 2% to 61%.

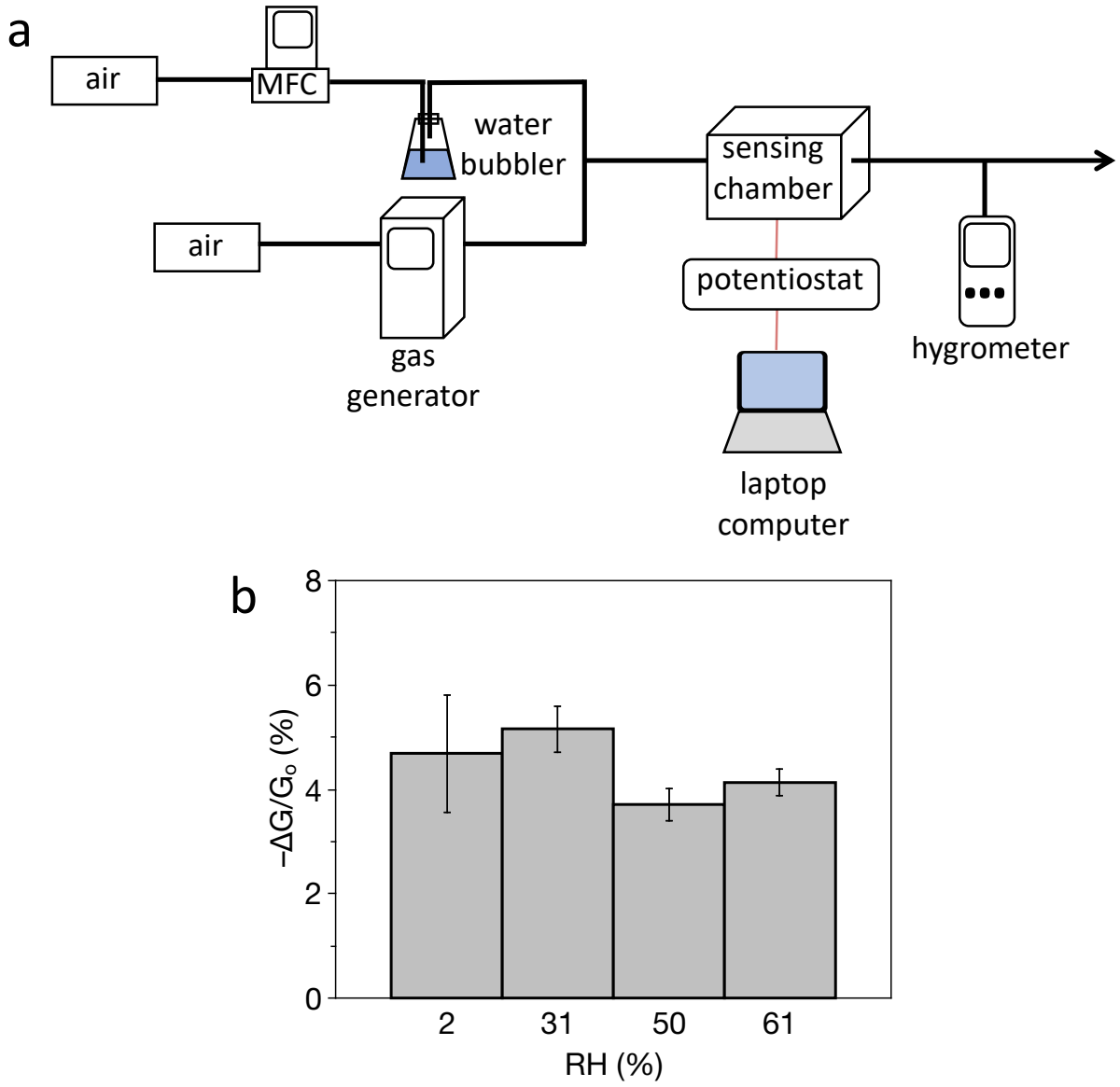

Figure S8. (a) Controlled humidity gas sensing setup. (b) Response of sensors to 60 s of 5 ppm NDMA exposure from low relative humidity (2%) to high relative humidity (61%).

11. Detection of NDEA and NDBA

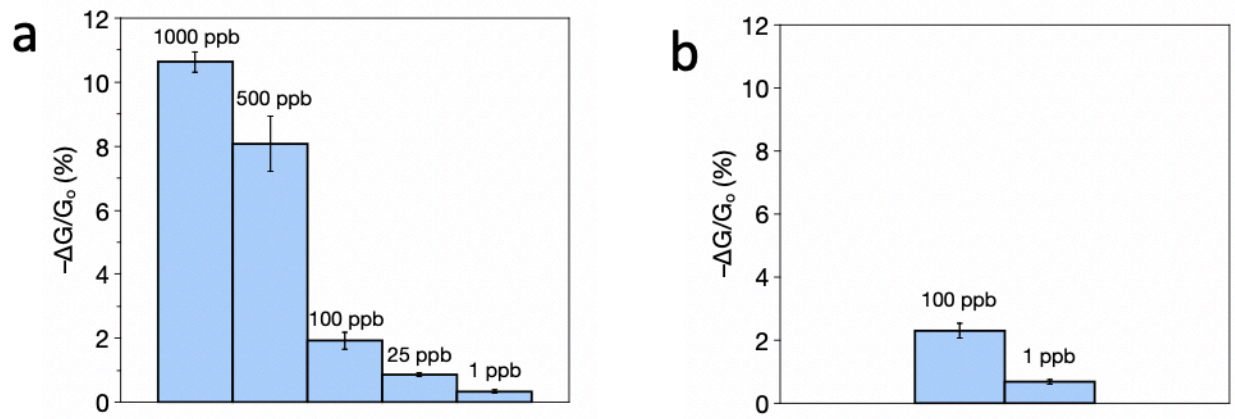

Figure S9. Response of Cobalt (III) porphyrin-4Py-(7,6)-SWCNTs sensors to 20 min exposure of (**a**) various ppb levels of NDBA and (**b**) 100 ppb and 1 ppb of NDEA in air.

12. Sensing setup with commercial sensing node

Sensing with a commercial sensing node was carried out using a C2Sense SensingNode. A glass gold electrode prepared with sensing material deposited on 300 μm gap working electrodes were inserted into the sensing cartridge and fitted into the sensing node. Gaseous analytes were introduced to the sensing node by drawing ~100 mL/min gas from the gas generator using its internal pump (**Figure S10**). The sensing node was wirelessly connected to a TP-Link WiFi router and controlled by the C2Sense Node Control web page using a web browser on a computer or a cell phone. The resistance of the sensors was recorded and converted to response by $-\Delta G/G_o$ (%) = $(R_o - R)/R_o \times 100\%$, where R_o is the initial resistance.

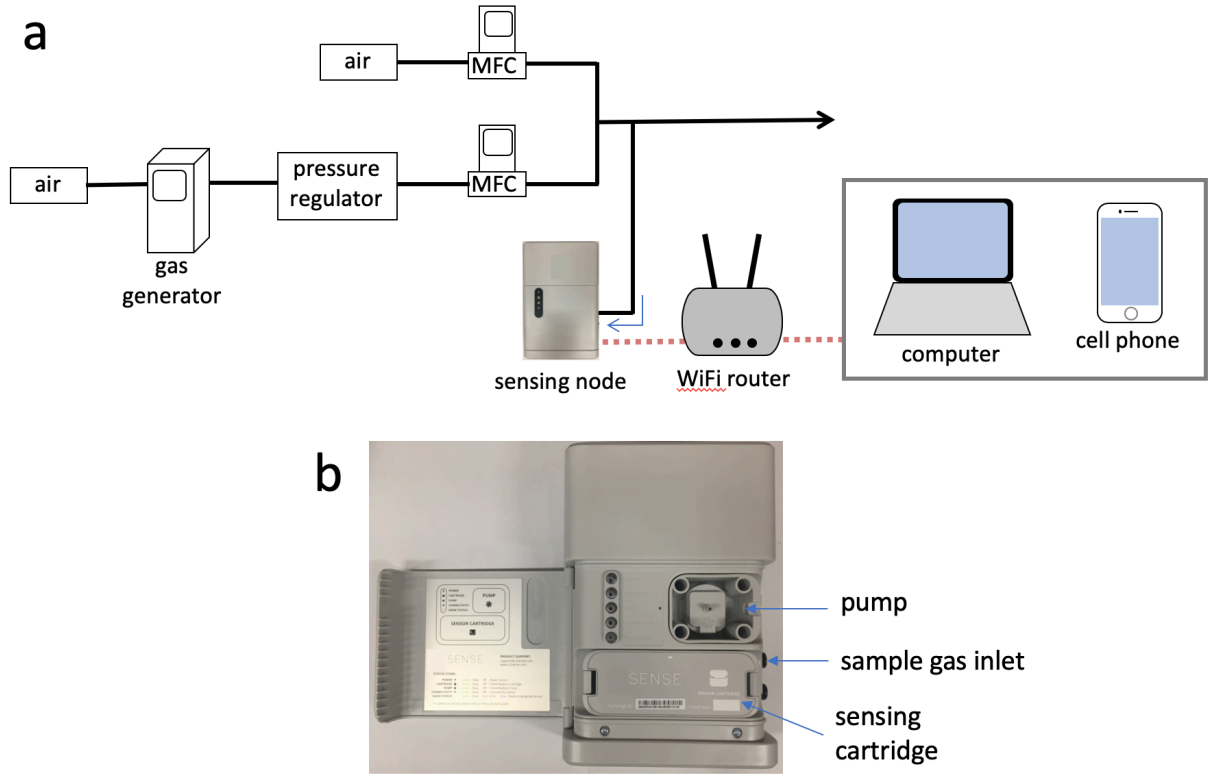

Figure S10. (**a**) Sampling of gas into a sensing node. (**b**) C2Sense SensingNode.

13. Reversibility of sensors

The degree of reversibility of Cobalt (III) tetraphenyl porphyrin and 4Py-(7,6)-SWCNTs sensors is shown in **Figure S11**. The sensors were exposed to 60 s of 200 ppm of NDMA in air.

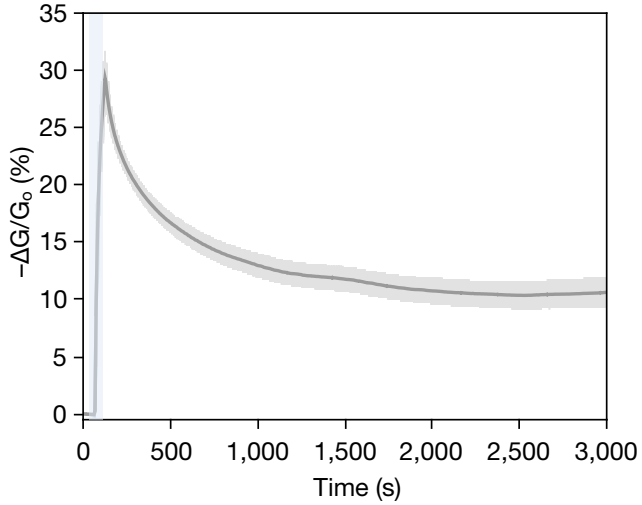

Figure S11. Sensor reversibility. The area highlighted in light blue indicates exposure to NDMA.

14. References

(1) Heath, D. F.; Mattocks, A. R. 823. Preparation of 14C-Labelled Dialkylnitrosamines, and an Improved Preparation of N-Methyl-N-t-Butylamine. *J. Chem. Soc.* **1961**, 4226–4229.

(2) Karabatsos, G. J.; Taller, R. A. Structural Studies by Nuclear Magnetic Resonance. IX. Configurations and Conformations of N-Nitrosamines. *J. Am. Chem. Soc.* **1964**, *86* (20), 4373–4378.

(3) Lunn, G.; Sansone, E. B. *Destruction of Hazardous Chemicals in the Laboratory*; John Wiley & Sons, Inc.: Hoboken, NJ, USA, 2012.

(4) Savagatrup, S.; Schroeder, V.; He, X.; Lin, S.; He, M.; Yassine, O.; Salama, K. N.; Zhang, X.-X.; Swager, T. M. Bio-Inspired Carbon Monoxide Sensors with Voltage-Activated Sensitivity. *Angew. Chemie Int. Ed.* **2017**, *56* (45), 14066–14070.

(5) He, M.; Swager, T. M. Covalent Functionalization of Carbon Nanomaterials with Iodonium Salts. *Chem. Mater.* **2016**, *28* (23), 8542–8549.

(6) Adler, A. D.; Longo, F. R.; Kampas, F.; Kim, J. On the Preparation of Metalloporphyrins. *J. Inorg. Nucl. Chem.* **1970**, *32* (7), 2443–2445.

(7) Summerville, D. A.; Jones, R. D.; Hoffman, B. M.; Basolo, F. Chromium(III) Porphyrins. Chemical and Spectroscopic Properties of Chloro-Meso-Tetraphenylporphinatochromium(III) in Nonaqueous Solutions. *J. Am. Chem. Soc.* **1977**, *99* (25), 8195–8202.

(8) Okada, K.; Sumida, A.; Inagaki, R.; Inamo, M. Effect of the Axial Halogen Ligand on the Substitution Reactions of Chromium(III) Porphyrin Complex. *Inorganica Chim. Acta* **2012**, *392*, 473–477.

(9) Hill, C. L.; Williamson, M. M. Structural and Electronic Properties of Six-Coordinate Manganese(III) Porphyrin Cations. Crystal and Molecular Structure of Bis(N,N-Dimethylformamide)(Tetraphenylporphinato)Manganese(III) Perchlorate, [MnIII TPP(DMF)2]+ClO4-. *Inorg. Chem.* **1985**, *24* (18), 2836–2841.

(10) Scheidt, W. R.; Cohen, I. A.; Kastner, M. E. A Structural Model for Heme in High-Spin Ferric Hemoproteins. Iron Atom Centering, Porphinato Core Expansion, and Molecular Stereochemistry of High-Spin Diaquo(Meso-Tetraphenylporphinato)Iron(III) Perchlorate. *Biochemistry* **1979**, *18* (16), 3546–3552.

(11) Sonkar, P. K.; Prakash, K.; Yadav, M.; Ganesan, V.; Sankar, M.; Gupta, R.; Yadav, D. K. Co(II)-Porphyrin-Decorated Carbon Nanotubes as Catalysts for Oxygen Reduction Reactions: An Approach for Fuel Cell Improvement. *J. Mater. Chem. A* **2017**, *5* (13), 6263–6276.
(12) Sugimoto, H.; Ueda, N.; Mori, M. Preparation and Physicochemical Properties of Tervalent Cobalt Complexes of Porphyrins. *Bull. Chem. Soc. Jpn.* **1981**, *54* (11), 3425–3432.
(13) Vail, S. A.; Schuster, D. I.; Guldi, D. M.; Isosomppi, M.; Tkachenko, N.; Lemmetyinen, H.; Palkar, A.; Echegoyen, L.; Chen, X.; Zhang, J. Z. H. Energy and Electron Transfer in β-Alkynyl-Linked Porphyrin-[60] Fullerene Dyads. *J. Phys. Chem. B* **2006**, *110* (29), 14155–14166.
(14) Liu, S. F.; Moh, L. C. H.; Swager, T. M. Single-Walled Carbon Nanotube–Metalloporphyrin Chemiresistive Gas Sensor Arrays for Volatile Organic Compounds. *Chem. Mater.* **2015**, *27* (10), 3560–3563.
(15) Lunn, G.; Sansone, E. B.; Keefer, L. K. Safe Disposal of Carcinogenic Nitrosamines. *Carcinogenesis* **1983**, *4* (3), 315–319.